

# Chapter 19

## Wavenumber Decomposition Applied to a Negative Impedance Shunts for Vibration Suppression on a Plate

F. Tateo, K.A. Cunefare, M. Collet, and M. Ouisse

**Abstract** In the last few decades, researchers have given a lot of attention to new engineered materials with the purpose of developing new technologies and devices such as mechanical filters, low frequency sound and vibration isolators and acoustic waveguides. So-called metamaterials are an example of such, where apparent material properties are engineered into structures by exploiting periodicity as well as active and passive elements to achieve desired ends.

This paper explores the active vibration control performance of such a metamaterial, considered as a metacomposite comprising an active interface between two regions of an extended aluminum plate; one region has a disturbance input while the other region is meant to be protected by the active interface.

The active interface is a 75-element array of piezoelectric patches individually connected to synthetic negative capacitance control circuits. The performance is analyzed through a wavenumber decomposition of the velocity field in the wavenumber domain. The wavenumber decomposition is applied to each region individually, as well as to the entire plate. The wavenumber decomposition also provides insight into the potential control of radiated noise from the structure.

**Keywords** Negative capacitance • Semi-active vibration control • Smart materials • Wavenumber domain filtering • Metacomposites

### 19.1 Introduction

The design of innovative structures incorporating multiple physical functionalities represents a big challenge for both industrial and academic communities. This paper is a contribution to the challenges of designing and implementing a new class of integrated smart metacomposites capable of improved engineering performances in terms of mechanical and vibroacoustic behavior as compared to strictly passive structures.

The definition of a metacomposite combines two different aspects of vibration control:

- The first aspect is connected to periodic structure theories, which are usually associated with metamaterial developments.
- The second concept includes the definition of composite conceived in a broader sense, in which shunted piezoelectric materials, electronic components, controllers and the structure are intimately connected to each other.

The concept of metacomposite is therefore associated to the notion of programmable matter coined by Toffoli [6] to refer to an ensemble of computing elements arranged in space is now extended to smart materials based on distributed piezoelectric actuators able to modify the inherent vibroacoustic properties based on an input signal.

---

F. Tateo (✉) • M. Collet • M. Ouisse  
Department of Applied Mechanics, Femto-st, Besançon, France  
e-mail: [flaviano.tateo@femto-st.fr](mailto:flaviano.tateo@femto-st.fr)

K.A. Cunefare  
School of Mechanical Engineering, Georgia Institute of Technology, Atlanta, GA, USA

M. Collet  
LTDS, Ecole Centrale de Lyon, Ecully, France

Over the years different solutions including such a new material have been proposed. To cite a few, in the field of light propagation, research has explored how to design and construct photonic crystals exhibiting photonic band gaps that prevent light from propagating in certain directions with specified frequencies. Other efforts have explored creation of photonic crystals able to propagate light in anomalous and useful ways [3]. In the acoustic domain, similar studies were carried out with the aim of preventing the propagation of elastic waves within a medium. For both light and acoustic waves, the band gap is obtained by periodically modulating some electromagnetic or mechanical properties [7].

This technique presents two main problems:

- the spatial modulation must be of the same order as the wavelength in the gap,
- the position of the band gap cannot be easily changed since it strongly depends on the materials employed (Bragg's band gap).

A possible solution for these problems is found using composites with locally resonant units. The periodicity of the crystal creates a stop band that can be shifted by modifying the properties of the resonators [4]. The same idea was extended in the vibroacoustic domain for the control of elastic waves propagating into a waveguide. The resonant units in this case were obtained using RL circuits shunted to piezoelectric ceramics embedded on the structure's surface. An elegant formulation of passive shunting was first proposed by Hagood and Von Flotow [2] and is still commonly used. The study showed how a piezoelectric material shunted through a series RL circuit, i.e., a resonant shunt, which would exhibit a behavior analogous to the well-known mechanical tuned mass damper. Periodically induced impedance-mismatch zones generate broader stop bands. The tunable characteristics of shunted piezo-patches allow the equivalent mechanical impedance of the structure to be tuned so that stop bands are generated over desired frequency ranges. The resistance allows the energy dissipation mechanism of shunted piezos to be exploited.

Eventually a broader control effect can be achieved by using negative capacitance shunts. In this configuration, a piezoelectric patch is shunted through a passive circuit to a synthetic negative impedance converter. In this way, the internal capacitance of the piezoelectric ceramic is artificially canceled and the impedance of the shunt circuit reduces to that of the passive circuit. Although the negative capacitance shunting strategy has been experimentally validated, it must be used with caution since it requires active elements that can destabilize the structure if improperly tuned. This technique requires in fact to tune the circuit very close to the stability limit.

In this paper, the metamaterial structure of interest consists of an array of piezoelectric patches periodically arranged over a limited region of the surface of a two-dimensional waveguide. This array of patches is intended to serve as an active interface between regions of the waveguide, formed from a plate. This active interface allows modification of the scattering properties of the waveguide in terms of reflected and absorbed energy. This controlling capability is obtained by correctly tuning the parameters of the external circuit by which almost arbitrary effective structural impedance may be obtained [1]. The novelty of the paper at hand is to use an array of periodic shunted patches to create a controllable impedance boundary between an upstream and downstream section of the two-dimensional plate waveguide.

The core of this work is to propose an experimental technique able to qualify the smart interface from the dynamic point of view. To do so a Scanning Laser Doppler Vibrometer (SLDV) is used to measure the velocity of the inspected surface in points belonging to a predefined grid. Scanning the grid and post-processing the data allows the detection and the visualization of the full wave-field as it propagates in the structure. The resulting images describe the main features of the propagating wave and show its interactions with discontinuities that may be encountered along the wave path.

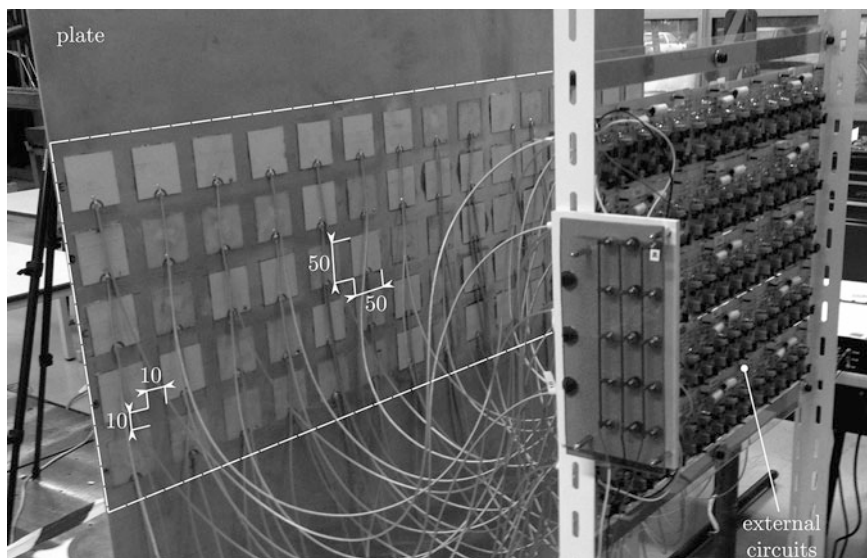
Thanks to this approach the smart metamaterial is analyzed and the performances of the control system are estimated.

## 19.2 Metacomposite Design

This section introduces the design of the smart metamaterial including the plate structure, the design criteria leading to selection of the piezoelectric patches used in the active interface and the design and impedance characteristics of the shunting circuit.

The basic structure of the metamaterial comprises an aluminum plate and an array of piezoelectric ceramics arranged in a periodic fashion. Each subcomponent have the following dimensions:  $2,100 \times 1,050 \times 3$  mm for the plate and  $50 \times 50 \times 0.5$  mm for the piezoelectric patch respectively. Regarding the mechanical properties the plate has a mass density of  $2,700 \text{ kg/m}^3$ , a Young's modulus of 70 GPa and a Poisson's ratio of 0.33. Each piezoelectric ceramic has a mass density of  $7,650 \text{ kg/m}^3$ , a Poisson's ratio of 0.31, dielectric loss smaller than 0.05 % and a coupling factor of 0.31. The plate is suspended from a rigid frame by metallic wires in order to approximate free-free boundary conditions. The plate is equipped with 75 piezoelectric patches (Ferroperm Industries P Z26 series) arranged in a regular  $15 \times 5$  array as seen in Fig. 19.1. The patches and the

**Fig. 19.1** Photograph of plate with 75 element piezoelectric patch array comprising an active interface, connected to bank of 75 individual negative impedance shunt control circuits



depth of the patch array were selected based on consideration of their size relative to the shortest structural wavelength of interest. The array was intended to be effective up to a frequency of 5,000 Hz. The plate's dispersion relation for the  $A_0$  flexural mode at 5,000 Hz has a wavelength of about 30 cm. With patches having dimensions of  $50 \times 50$  mm, there will be no charge cancellation on an individual patch as would occur if the patch dimensions were comparable to a wavelength. Further, the depth of the patch array is 350 mm such that it spans more than a wavelength at 5,000 Hz. Since the array elements are uncoupled electronically, each element within the array would still function at the highest frequency of interest, even though the entire array depth would be comparable to a wavelength. The thickness of the patch was selected considering the constraints of the electric circuit and the nature of the control technique. Different authors have shown that the best controlling effect is obtained when the negative impedance shut circuit is tuned close to the inherent patch capacitance. This property strongly depends on the material properties and the geometry of the patch. Once the material properties and the two dimensions of the piezoelectric patch are chosen, the only parameter which remains for selection is the thickness. Thin patches exhibit larger values of intrinsic capacitance which would yield increased control, however, this parameter cannot be reduced indefinitely due to the weakening of the piezoelectric patch itself. For these reasons, a thickness of 0.5 mm was selected.

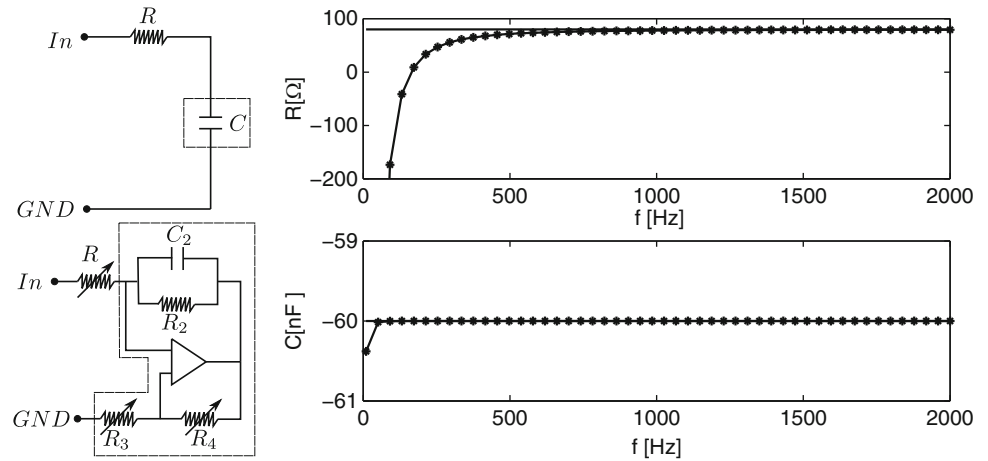
The controlling capability is obtained by properly tuning the external circuit an optimization procedure [1] has been used with the objective of identifying the real and the imaginary parts of an imposed synthetic impedance. Two possible behaviors depending on the criterion used in the optimization have been identified: minimizing the velocity of the energy propagation in the region of the active array it is therefore possible to limit the propagation of the wave beyond the active interface; choosing a criterion based on exploiting the effect of electrical damping it is possible to modify the dynamic properties of the plate by increasing the energy absorption properties of the active interface.

However, the required electrical impedances for these two circuit optimization approaches cannot be readily reproduced experimentally because it is not possible to exactly recreate the optimal resistance and capacitance over the whole frequency range of interest. For the work presented here, the layout of the actual circuit implemented for control of the patches is presented in Fig. 19.2. This circuit contains a number of passive components, including the resistances  $R$ ,  $R_2$ ,  $R_3$ ,  $R_4$  and the capacitance  $C_2$  as well as an active component, specifically, an operational amplifier that is essential for the circuit to reproduce the desired behavior. This specific circuit layout was chosen as opposed to others because of its simplicity and its effectiveness in the frequency range of interest. The impedance of the circuit in Fig. 19.2 is determined by the formula

$$Z_{eq}(\omega) = R - \frac{R_3 R_2}{R_4 (1 + i\omega R_2 C_2)} \quad (19.1)$$

Figure 19.2 depicts the frequency-dependent behavior of the actual impedance produced by the circuit; in the top of the figure is the equivalent resistance and at the bottom the equivalent capacitance. Both terms vary as a function of the frequency; in particular the resistance at low frequency presents a negative value that can introduce some instability which can degrade the overall performance of the control system. From the practical point of view, the circuit presented in Fig. 19.2 is further modified. The resistances  $R_3$  and  $R_4$  were implemented through a single potentiometer  $R_{pot}$  with the aim of simplifying the

**Fig. 19.2** Comparison between the desired performance of the ideal circuit and that of the physically implemented circuit. On the *left*, basic architecture of circuit; on the *right* the circuit's impedance depicted in terms of equivalent resistance (*top*) and equivalent capacitance (*bottom*)



circuit layout. The negative impedance control technique requires tuning of the synthetic capacitance around the capacitance value of the piezoelectric ceramic at free stress condition; this value is intrinsic to the electromechanical coupling and depends upon the material properties, the geometry of the patches and the plate stiffness. The intrinsic capacitance of the piezoelectric patch can be estimated by measurement using a capacitance meter when the specimen is free of external forces (in the case at hand 52 nF). The actual circuit was tuned by varying the position of the potentiometer  $R_{pot}$  in small increments from high negative values of the synthetic capacitance to a value very close to the intrinsic capacitance value.

### 19.3 Experimental Setup

The structure of interest, described in the previous section, consists of an aluminum plate equipped with 75 piezoelectric actuators connected to external circuits and arranged so as to form a periodic array of  $5 \times 15$  units. Standard epoxy glue was used to bond the piezoelectric ceramics to the top surface of the plate.

Elastic waves are excited by a shaker as depicted in Fig. 19.3. The input transducer, located in the lower part of the plate 840 mm away from the active interface (point  $E$ ), is driven by a sinusoidal burst generated by a signal generator and amplified by an LDS power amplifier. The resulting elastic waves are recorded at the measurement grid points. The operation of the scanning laser vibrometer (Polytec PSV-400) requires the generation of a pulse at each grid point in order to record the corresponding response. Phase information is retained by triggering the excitation signal through a low frequency signal, which also defines the scanning rate. Upon completion of measurements at all grid points, the recorded responses are then post-processed to obtain full images of the propagating wave-field within the region of inspection. A schematic of the set-up considered for wave-field measurement is shown in Fig. 19.3. Measurements were conducted over a grid of  $37 \times 81$  scan points with a spatial resolution of 20 mm in the horizontal and vertical directions. At each grid point, the laser measures the time history of the out-of-plane velocity

$$w_{3D} = w_{3D}(x, y, t). \quad (19.2)$$

Figure 19.4 presents the full-field velocity measurement obtained scanning the plate's surface with the laser beam. For each time step is possible to visualize the system response, after few  $ms$  some reflections due to the boundaries are observed the wave-field is clearly modified. This phenomenon can potentially create problems in the subsequent analysis since the interaction between the main wave-front and the reflections can generate undesired effects; the assumption of cylindrical waves freely propagating within the plate no longer applies.

### 19.4 Analysis of 2D Waveguide

In many applications guided waves are used in order to interrogate the integrity of a structure. In SHM application analysts need to isolate specific wave-modes associated to the reflections due to an obstacle (i.e. damage) from the global response. In these cases the nature of the propagating waves (direction, shape and amplitude) is modified. By simply analysing the raw data (time history) it is very hard to distinguish the different components associated to the propagating wave. In order

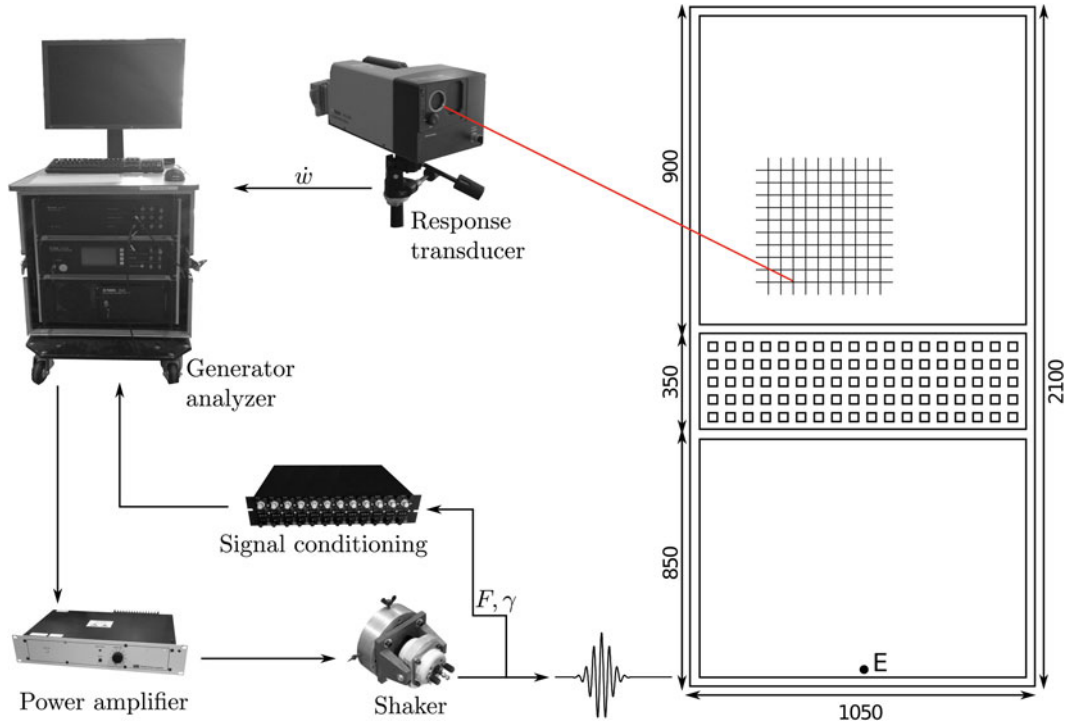


**Fig. 19.3** Schematic of the experimental set-up for wave-field measurement

to overcome this specific difficulty a filtering technique in the wave number domain is used with the purpose of separating the different wave-modes composing the measured response [5]. The approach described so far is extended to the smart metamaterial by just assuming that the active interface is able to modify the scattering properties of the simple waveguide (plate). The raw signal  $w_{3D}$  is first modified by just considering the spatial response of the system along the  $y$  direction

$$w_{2D} = w_{2D}(y, t) = w_{3D}(\bar{x}, y, t) \quad (19.3)$$

as depicted in Fig. 19.4 (white line).

The signal  $w_{2D}$  is then Fourier transformed

$$W_{2D} = W_{2D}(k_y, f) = \mathcal{F}_{2D}(w_{2D}(y, t)) \quad (19.4)$$

obtaining a frequency/wavenumber representation that can be used to effectively isolate the targeted wave-mode from the overall response which is a combination of the primary wave generated by the exciter and the waves associated to the reflection (i.e. boundaries).

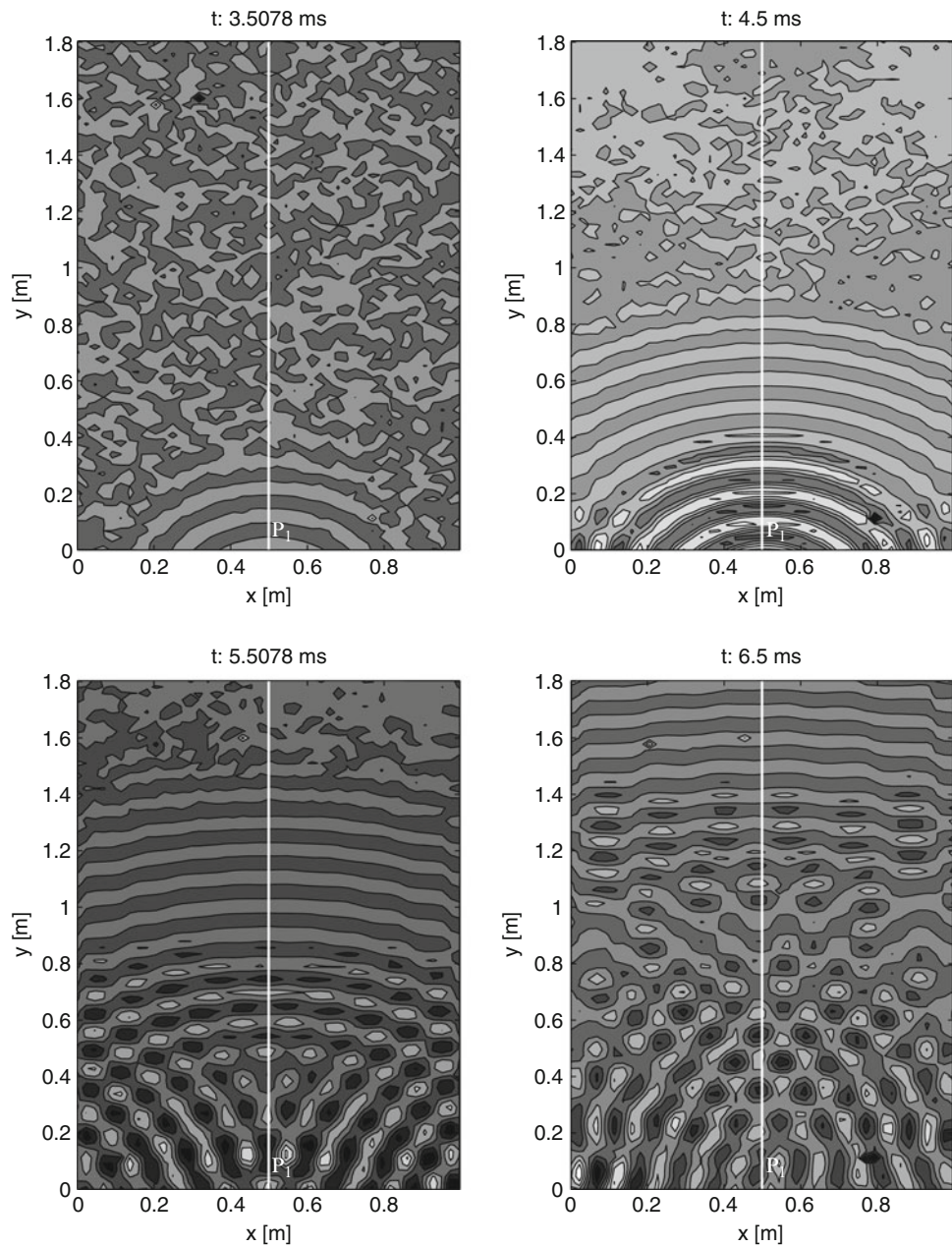
The 2D Fourier transform effectively separates the different wave components; by using a simple window functions is possible to filter out almost all the undesired components. The filtering procedure is based on the selection of the wave-modes having a dispersion relation (contour plot) similar to the theoretical dispersion relation associated to the bare plate (black line), as depicted in the top of Fig. 19.5.

Upon filtering, the residual signal can be transformed back through an inverse Fourier transform to the space/time domain for visualization and further processing. From this perspective, 2D Fourier transform based filtering represents an attractive approach to separate a given wave. Mathematically, the windowing process can be simply expressed as a function product between the wave's 2D Fourier transform and a 2D window function:

$$W_{2D}^* = H(k - k_0, \omega - \omega_0) W_{2D}(k, \omega) \quad (19.5)$$

where  $H(k - k_0, \omega - \omega_0)$  denotes the window centered at  $k_0, f_0$ . The process is depicted graphically in Fig. 19.5, which respectively show a Hanning window overlapped to the signal's 2D spectrum and the residual signal upon filtering. The space/time domain approximation of the filtered response  $w_{2D}^*$  is expressed as

**Fig. 19.4** Experimental full-field velocity measurement at different time steps. The lower images clearly indicates the presence of reflection occurred in correspondence of the boundaries



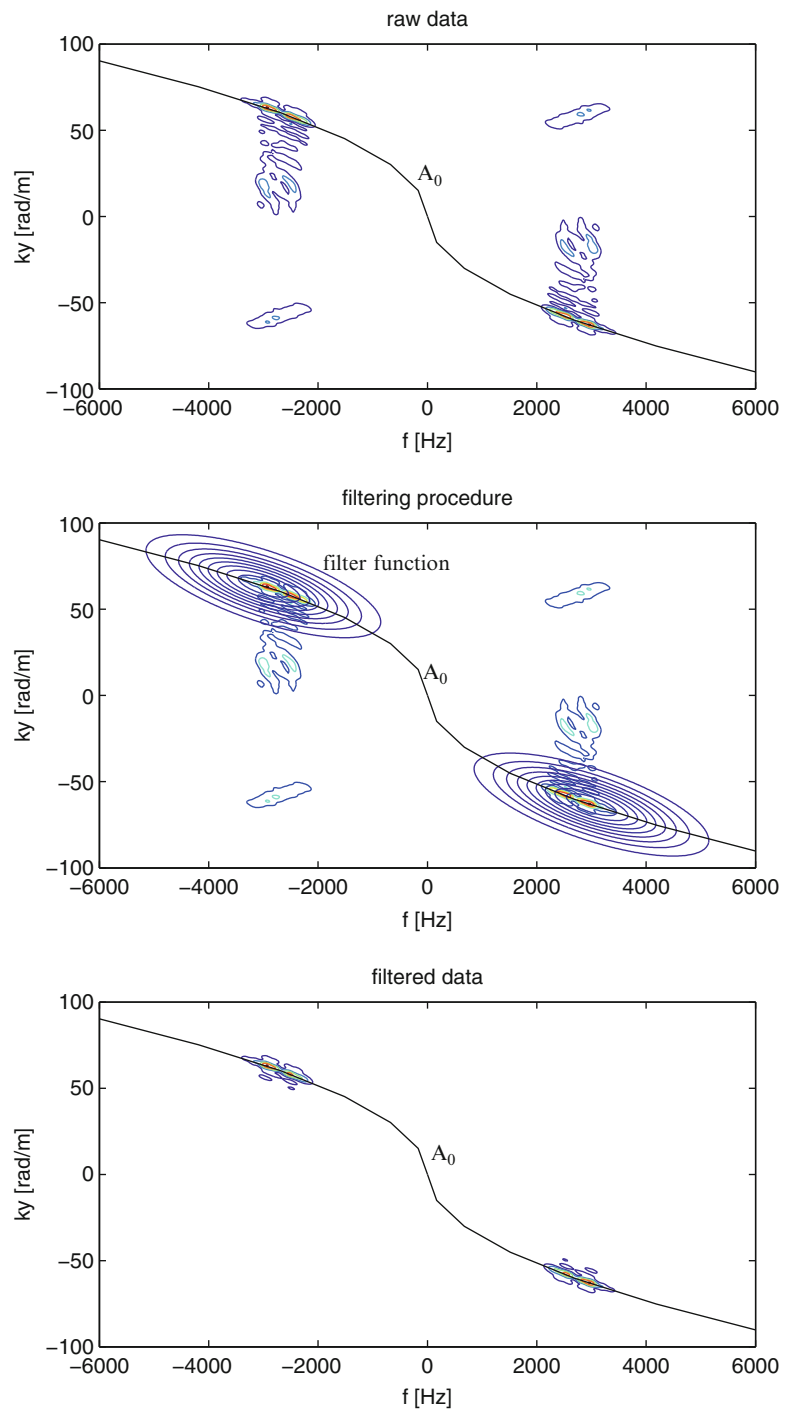
$$w_{2D}^*(x, t) = \mathcal{F}_{2D}^{-1}(W_{2D}^*(k, \omega)) \quad (19.6)$$

where  $\mathcal{F}_{2D}^{-1}$  denotes the inverse 2D Fourier transform.

The filtered signal  $w_{2D}^*$  is then Hilbert transformed in order to obtain the envelope of the response for each measurement's point belonging to the white line depicted in Fig. 19.4.

Comparing the response of the system presented in Fig. 19.6 for two different conditions: uncontrolled (left) and controlled (right) a modification in the response is observed. Figure 19.7 represents the spatial attenuation of the waves propagating within the metacomposite it associates the maxima of the filtered response to the spatial position along the  $y$  direction. The blue line represents the uncontrolled system whereas the green line represents the controlled system. By comparison it is clear that the external circuits is able to modify the dynamic behavior of the waveguide by adding an extra amount of damping.

**Fig. 19.5** Experimental vs. theoretical dispersion relations for the raw (*top*) and the filtered (*bottom*) signals. The image at the center represent the filter used in the wave number domain



## 19.5 Conclusions

This paper presents a signal processing technique aimed at improving the visualization capabilities of full wave-field measurements. The technique operates in the frequency/wavenumber domain, where the presence of defect can be observed from the main signal generated for inspection. Upon filtering, the residual signal obtained just considering the  $A_0$  mode highlights the modification of the dynamic properties of the waveguide due to the presence of the active interface.

**Fig. 19.6** Experimental contour plot obtained by performing an inverse Fourier transform of the filtered signal for each spatial position for the uncontrolled (*left*) and controlled (*right*) system. The *white lines* represent the maximum of the response

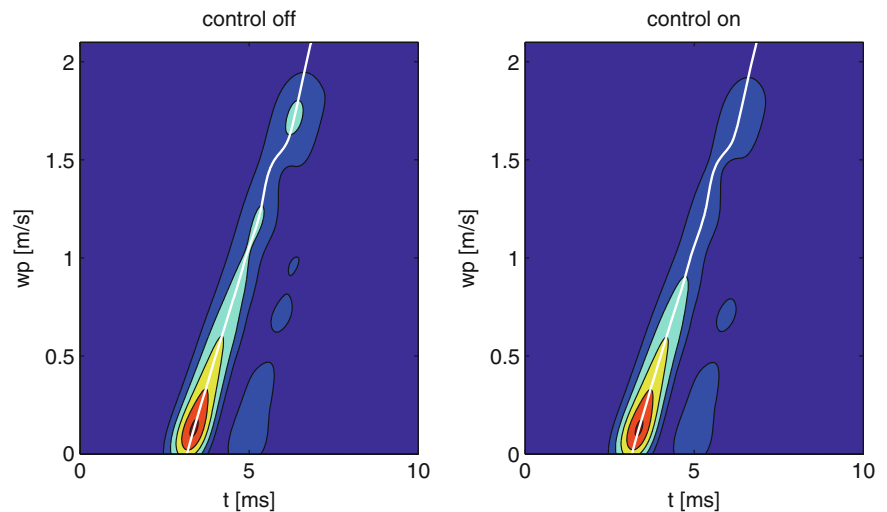
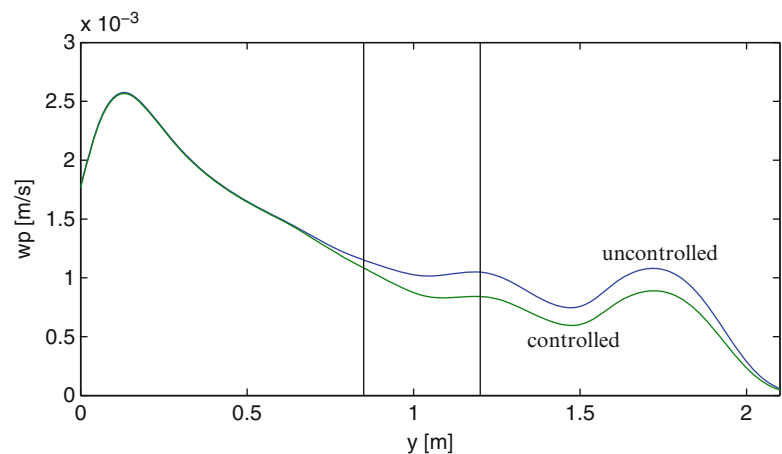


**Fig. 19.7** Spatial attenuation of the smart metacomposite: uncontrolled system (*blue line*); controlled system (*green line*) (Color figure online)



The presented results demonstrate the potential of the method and highlight future research needs. In particular, this method needs to be supported by a suitable technique able to suppress the effect related to the parasitic components associated to the boundaries reflections. This point is currently under investigation, by using a source images approach better results are expected.

## References

1. Collet M, Ouisse M, Ichchou MN (2012) Structural energy flow optimization through adaptive shunted piezoelectric metacomposites. *J Intell Mater Syst Struct* 23(15):1661–1677
2. Hagood NW, von Flotow A (1991) Damping of structural vibrations with piezoelectric materials and passive electrical networks. *J Sound Vib* 146(2):243–268
3. Joannopoulos JD, Johnson SG, Winn JN, Meade RD (2008) Photonic crystals: molding the flow of light. Princeton University Press, Princeton
4. Liu Z, Zhang X, Mao Y, Zhu YY, Yang Z, Chan CT, Sheng P (2000) Locally resonant sonic materials. *Science* 289(5485):1734–1736
5. Michaels TE, Michaels JE, Ruzzene M (2011) Frequency-wavenumber domain analysis of guided wavefields. *Ultrasonics* 51(4):452–466
6. Toffoli T, Margolus N (1991) Programmable matter: Concepts and realization. *Phys D Nonlinear Phenom* 47(1–2):263–272
7. Yang S, Page JH, Liu Z, Cowan ML, Chan CT, Sheng P (2002) Ultrasound tunneling through 3D phononic crystals. *Phys Rev Lett* 88(10):104301